

Confirmation of random matrix model for the antenna array channel by indoor measurements

Ralf R. Müller and Helmut Hofstetter*

Forschungszentrum Telekommunikation Wien (FTW), Vienna, Austria

Abstract — A random matrix model for communication via antenna arrays introduced recently in [1] characterizes the space-time nature of the channel in terms of the asymptotic eigenvalue distribution of its space-time covariance matrix as a function of the number of transmit antennas, receive antennas, and significantly scattering objects. This paper finds the theoretical predictions in [1] to accurately match data obtained in a recent measurement campaign. The number of significant scattering objects is found to strongly vary with frequency. The latter effect is described by the newly introduced richness spectrum.

I. INTRODUCTION

Communication via antenna arrays allows for a significant increase in spectral efficiency [2]. Several recent proposals [2, 3, 4] are aiming to utilize this advantage in various ways while the physical nature of such multiple-input multiple-output (MIMO) channels is still not fully understood.

Recently, a new model to describe the conditions for communication on such channels has been derived from random matrix and free probability [5] theory in [1]. Since it reduces the description of the propagation conditions to the distribution of the eigenvalues of the channel's covariance matrices, it provides a direct link from the physical environment, which it comprehensively parameterizes by the number of significantly scattering objects, to the standard performance measures in communication theory, such as channel capacity or signal-to-interference-and-noise ratios for various types of signal processing at receiver site.

Since the random matrix model proposed in [1], includes several assumptions made for sake of analytical tractability, the question how accurate it models real-world scenarios seems important. In this paper, data obtained from indoor measurements of MIMO channels are found to accurately match the theoretical predictions in [1] and show large deviations to earlier random matrix models reported in [6, 7]. For convenience of the reader, the proposed model is briefly summarized in the following section.

II. CHANNEL MODEL

Consider a communication link with T transmit and R receive antennas. Let there be S_{\max} scattering objects each corresponding to a propagation path with excess delay τ_κ . Then, the signal that is received at antenna ν is given by

$$y_\nu(t) = \sum_{\kappa=1}^{S_{\max}} A_\kappa e^{j\varphi_{\kappa,\nu}} \sum_{\mu=1}^T e^{j\vartheta_{\kappa,\mu}} x_\mu(t - \tau_\kappa) \quad (1)$$

where $x_\mu(t)$ is the signal transmitted at antenna μ and $\varphi_{\kappa,\nu}$, $\vartheta_{\kappa,\mu}$, and A_κ are the relative carrier phases at the ν^{th} receive and μ^{th} transmit antenna and the attenuation of the κ^{th} path, resp.

Paths whose delays are not sufficiently separated in time cannot be resolved at the receiver. Thus, all paths are grouped in ascending order of their respective delays into L disjoint sets \mathcal{D}_ℓ such that all paths with similar delays form one set. Then, (1) can be decomposed into

$$y_\nu(t) = \sum_{\ell=0}^{L-1} \sum_{\kappa \in \mathcal{D}_\ell} A_\kappa e^{j\varphi_{\kappa,\nu}} \sum_{\mu=1}^T e^{j\vartheta_{\kappa,\mu}} x_\mu(t - \tau_\kappa).$$

Thus, the propagation coefficient from antenna μ to antenna ν at the delay associated with index ℓ is given as

$$h_{\nu,\mu,\ell} = \sum_{\kappa \in \mathcal{D}_\ell} A_\kappa e^{j(\vartheta_{\kappa,\mu} + \varphi_{\kappa,\nu})}. \quad (2)$$

The number of scatterers may vary with delay. Therefore, it is sensible to model this effect by the scatterer count delay profile [1] $S_\ell \triangleq |\mathcal{D}_\ell|$ in addition to the well-known power-delay profile

$$P_\ell \triangleq \frac{1}{R} \sum_{\kappa \in \mathcal{D}_\ell} |A_\kappa|^2. \quad (3)$$

The received signal at fixed delay may be written in vector notation as $\mathbf{y}_\ell = \mathbf{H}_\ell \mathbf{x}$ where the entries of the $R \times T$ matrix \mathbf{H}_ℓ are defined in (2). It is obvious from (2) that those entries show strong statistical dependencies even if A_κ , $e^{j\vartheta_{\kappa,\mu}}$, and $e^{j\varphi_{\kappa,\nu}}$ are statistically independent for all κ , μ , and ν .

Let $\mathcal{D}_\ell = \{1, \dots, S_\ell\}$. Define the matrices

$$\mathbf{\Theta}_\ell \triangleq \begin{bmatrix} e^{j\vartheta_{1,1}} & \dots & e^{j\vartheta_{1,T}} \\ \vdots & \ddots & \vdots \\ e^{j\vartheta_{S_\ell,1}} & \dots & e^{j\vartheta_{S_\ell,T}} \end{bmatrix}, \quad (4)$$

$$\mathbf{\Phi}_\ell \triangleq \begin{bmatrix} e^{-j\varphi_{1,1}} & \dots & e^{-j\varphi_{1,R}} \\ \vdots & \ddots & \vdots \\ e^{-j\varphi_{S_\ell,1}} & \dots & e^{-j\varphi_{S_\ell,R}} \end{bmatrix}, \quad (5)$$

and $\mathbf{A}_\ell \triangleq \text{diag}([A_1, \dots, A_{S_\ell}])$. Then, \mathbf{H}_ℓ may be expressed as

$$\mathbf{H}_\ell = \mathbf{\Phi}_\ell^H \mathbf{A}_\ell \mathbf{\Theta}_\ell. \quad (6)$$

If there is no line of sight and the antennas within the transmitter array are spaced sufficiently far apart from each other, it is reasonable to assume that the entries within the matrices $\mathbf{\Theta}_\ell$ are statistically independent random variables. A corresponding statement holds for the receiver array and the matrices $\mathbf{\Phi}_\ell$. Physical measurements strongly indicate that the correlation between the direction of arrival and the

$$\begin{bmatrix} \vdots \\ \mathbf{y}[0] \\ \mathbf{y}[1] \\ \vdots \end{bmatrix} = \underbrace{\begin{bmatrix} \ddots & \ddots & \ddots & \ddots & \ddots & \ddots & \ddots & \ddots & \ddots \\ \cdots & \mathbf{0} & \mathbf{H}_{L-1} & \cdots & \mathbf{H}_1 & \mathbf{H}_0 & \mathbf{0} & \cdots & \cdots \\ \cdots & \cdots & \mathbf{0} & \mathbf{H}_{L-1} & \cdots & \mathbf{H}_1 & \mathbf{H}_0 & \mathbf{0} & \cdots \\ & & & \ddots & \ddots & \ddots & \ddots & \ddots & \ddots \end{bmatrix}}_{\triangleq \mathcal{H}} \begin{bmatrix} \vdots \\ \mathbf{x}[0] \\ \mathbf{x}[1] \\ \vdots \end{bmatrix} \quad (7)$$

direction of departure are negligible [8]. Therefore, we also assume Θ_ℓ and Φ_ℓ to be mutually statistically independent.

The propagation in time is described in matrix algebra by a space-time channel matrix (7) where the matrix-valued symbols $\mathbf{x}[k]$ and $\mathbf{y}[k]$ at transmitter and receiver site, resp., sent at subsequent time instances k are stacked into a single vector each.

Theorem 1 [1] *Let $T, R, S_\ell \rightarrow \infty$, but the ratios*

$$\beta \triangleq \frac{T}{R} \quad \text{and} \quad \zeta \triangleq \frac{T}{S_{\max}} \quad (8)$$

remain fixed. Moreover, let the power delay profile be constant, i.e. $\mathbf{A}_\ell = \mathbf{I}$, then the normalized moments of the space-time covariance matrix $\mathcal{H}^H \mathcal{H}$ converge in probability to [1]

$$m_n(\beta, \zeta) \triangleq \frac{\text{trace}(\mathcal{H}^H \mathcal{H})^n}{\text{trace}(\mathcal{H}^H \mathcal{H})} = \quad (9)$$

$$\sum_{i=0}^{n-1} \sum_{j=0}^{n-1} \binom{n}{i} \binom{n}{j} \binom{n}{i+j+1} \frac{\beta^i \zeta^j}{n}.$$

The parameters β and ζ are called *system load* and *channel load* [1]. Note that, the moments in (9) are also the moments of the respective eigenvalue distribution

$$m_n(\beta, \zeta) = \lim_{|\mathcal{E}| \rightarrow \infty} \frac{1}{|\mathcal{E}|} \sum_{\lambda \in \mathcal{E}} \lambda^n$$

with \mathcal{E} denoting the set of eigenvalues of the space time covariance matrix.

III. COMPARISON TO MEASUREMENTS

Previously, several assumptions, i.e. asymptotically large arrays, constant power delay profile, statistical independence among the entries of Φ and Θ , etc., have been made. The motivation behind these assumptions was analytical tractability. Moments calculated under such idealized assumptions are not sure to adequately match eigenvalue statistics experienced in practice. This section provides a comparison between the moments of the eigenvalue distributions of space-time channels matrices calculated from the channel model proposed in Section II to those ones observed in an indoor measurement campaign with the vector channel sounder RUSK-ATM manufactured by Medav GmbH.

All measurements mentioned in the following were recorded with a bandwidth of 120 MHz around a carrier frequency of 2 GHz. The receiver was an 8-element linear patch array spaced at half a wavelength. The transmitter was a single omni-directional antenna that was re-located by software control over a straight line in steps of half a wavelength. The patch

array was directed in such a way that line-of-sight was blocked.

The raw data provided by the vector channel sounder RUSK-ATM are matrix-valued complex frequency responses of the antenna array channel. The comparison to the theoretical predictions is based on the moments of the eigenvalue distribution given in (9). Following the reasoning in [1], the moments can be extracted from the measured data by

$$\hat{m}_n = \frac{\int_{1.94 \text{ GHz}}^{2.06 \text{ GHz}} \text{trace}(\mathbf{H}^H(f) \mathbf{H}(f))^n df}{\int_{1.94 \text{ GHz}}^{2.06 \text{ GHz}} \text{trace}(\mathbf{H}^H(f) \mathbf{H}(f)) df} \quad (10)$$

where $\mathbf{H}(f)$ and \hat{m}_n denote the matrix-valued frequency response and the measured n^{th} moment, resp.

Space-Time Measurements: For the first measurement described in this paper, the receiver was located in the author's office while the transmitter was placed in an adjacent room. The moments of the eigenvalue distribution obtained from this measurement via (10) are given in the first row of Tab. 1. For comparison, the moments calculated under the assumption of $S_{\max} = 6$ scattering objects of unit power using (9) are given in the second row of Tab. 1. The accurate fit of the calculated and measured moments give rise to the assumption that there actually happened to be 6 dominant scattering objects.

In order to investigate the influence of scattering objects, we stucked 35 pieces of scrambled tin foil, about $\frac{1}{2}$ to 1 m² in size, onto the walls, floors, ceilings, and furniture close to either receiver or transmitter. The moments measured from the same antenna positions with the help of tin foil are given in the third row of Tab. 1. They accurately match those moments calculated from (9) under the assumption of $S_{\max} = 30$ scattering objects of unit power, cf. fourth row in Tab. 1. For comparison, the fifth row of Tab. 1 shows the moments calculated from the probability density function of the eigenvalues of a covariance matrix that results from an 8×8 channel matrix with independent complex Gaussian entries reported in [6]. While reference [6] is able to model the finite size of the antenna array, it assumes independent identically distributed (i.i.d.) entries. The latter assumption, however, has turned out to be the critical one, while the absolute number of elements is less important.

The close fit between the theoretical predictions and the actual measurements in Tab. 1 are

$R = T = 8$	$\bar{\lambda}$	$\bar{\lambda}^2$	$\bar{\lambda}^3$	$\bar{\lambda}^4$	$\bar{\lambda}^5$	$\bar{\lambda}^6$	$\bar{\lambda}^7$	$\bar{\lambda}^8$
measured without tin foil	1.00	3.32	14.7	74.2	406	2.34k	14.0k	86.5k
calculated for $\zeta = 8/6$	1.00	3.33	14.8	75.0	413	2.39k	14.4k	88.8k
measured with tin foil	1.00	2.34	6.96	23.0	81.4	301	1.16k	4.56k
calculated for $\zeta = 8/30$	1.00	2.27	6.67	22.3	80.8	307	1.21k	4.92k
i.i.d. [6]	1.00	2.00	5.02	14.2	43.1	139	466	1.62k

Tab. 1: Moments of eigenvalue distributions. Measured in the author's office without tin foil, calculated for $S_{\max} = 6$, measured with tin foil, calculated for $S_{\max} = 30$, and under i.i.d. assumption, resp.

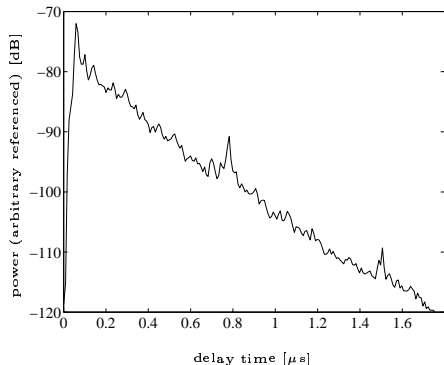


Fig. 1: Power delay profile in factory hall.

a convincing confirmation for the random matrix model for antenna array channels introduced in [1]. Note that the estimation of higher order moments of a distribution is a rather difficult task in practice. Therefore, the close match in Tab. 1 is very convincing.

The moments calculated by (9) refer to equal path loss for any scattering object. This assumption is well justified for an almost constant power delay profile. It is also justified as long as the number of dominant scattering objects is not much smaller than the number of antenna elements on either side. The latter condition is not straightforward. Therefore, it is explained in greater detail in the following: There are not more non-zero eigenvalues than $\min\{R, T\}$. Thus, only the $\min\{R, T\}$ most powerful scatterers show significant influence onto the eigenvalue distribution. Note that for higher order moments the power imbalances are more and more amplified.

In order to give a fair comparison, moments of eigenvalue distributions of channel covariance matrices are measured under propagation conditions which do not allow for negligence of power imbalances. Such a situation was found in a large factory hall (about 120 m \times 120 m) where the larger delays created the power delay profile shown in Fig. 1. The measurements show exponential decay of the impulse response over delay with a time constant of 180 ns. The newly introduced COST259 channel model [9] gives an estimated time constant of 360 ns for the factory hall scenario which is not confirmed by measurements and seems to be too large. Based on our measurements we recommend a time constant of 150 to 200 ns for the factory hall scenario. The moments measured in the factory hall are shown in the first row of Tab. 2. The second row of Tab. 2 shows the moments calculated via (9) for $S_{\max} = 3$ unit power scatterers which

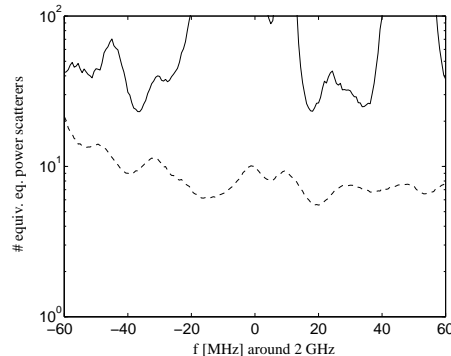


Fig. 2: Measured richness spectrum with and without tin foil shown by the solid and dashed line, resp.

turned out to fit best to the measured data. It can be observed that the fit is not as good as in Tab. 1, but by far better than with the i.i.d. assumption. Note also that the relative deviation is largest for the lower order moments. For those ones, the measured values are lower indicating more than 3 scatterers. Since these additional scatterers are received less powerful, their influence vanishes more and more at higher order moments.

Frequency Selectivity: In order to examine the behavior of the number of significant scattering objects over a wide frequency range, the number of equivalent equal power scatterers (EEPS) is extracted from the measurements. For this purpose, the moments at a particular frequency f are extracted from the measured matrix-valued transfer function in almost the same way as in (10), but without integration over a wide frequency range

$$\hat{m}_n(f) = \frac{\text{trace}(\mathbf{H}^H(f)\mathbf{H}(f))^n}{\text{trace}(\mathbf{H}^H(f)\mathbf{H}(f))}. \quad (11)$$

For the first N moments in (11), that channel load $\hat{\zeta}_N(f)$ is found that results in the smallest relative error to a set of moments that is allowed by random matrix theory, i.e.

$$\hat{\zeta}_N(f) = \underset{\zeta}{\text{argmin}} \frac{1}{N} \sum_{n=1}^N \left| \frac{m_n(\frac{T}{R}, \zeta)}{\hat{m}_n(f)} - 1 \right|. \quad (12)$$

From the channel load in (12), the richness spectrum

$$\hat{S}_N(f) \triangleq T/\hat{\zeta}_N(f) \quad (13)$$

is obtained. It is depicted for the measurement in the authors' office, cf. Tab. 1, in Fig. 2. It can be observed that the number of EEPS strongly depends on frequency. The maximum relative error compared to the model averaged over the first eight moments is 25% and 14% with and without tin foil, resp.

$R = 8, T = 15$	$\bar{\lambda}$	$\bar{\lambda}^2$	$\bar{\lambda}^3$	$\bar{\lambda}^4$	$\bar{\lambda}^5$	$\bar{\lambda}^6$	$\bar{\lambda}^7$	$\bar{\lambda}^8$
measured	1.00	6.42	61.3	697	8.88k	123k	1.83M	28.6M
calculated	1.00	7.88	78.3	882	10.7k	137k	1.82M	24.7M
i.i.d. [6]	1.00	2.87	10.2	40.2	171	762	3.54k	17.0k

Tab. 2: Moments of eigenvalue distributions. Measured in a factory hall, calculated for $S_{\max} = 3$, and under i.i.d. assumption, resp.

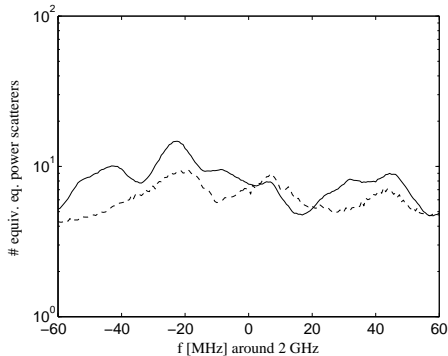


Fig. 3: Measured richness spectrum as in Fig. 2, but at shifted position of transmitter array.

Interestingly, it does not only strongly depend on frequency, but also on location: This effect was observed repeating the previous measurement with a uniform linear transmitter array shifted 3.5 wavelengths sideward. At that position, the richness spectrum depicted in Fig. 3

has been measured. The maximum relative error averaged over the first eight moments is 15% for both cases. Here, the addition of tin foil does not affect the number of EEPS significantly, although it is still slightly increased.

The strong dependency of the number of EEPS on frequency and position can be explained in the following way: At any scattering object several waves interfere, as the scatterers are larger than the wavelength. The exact position of the transmitter and the exact frequency of the wave determines whether the waves interfere constructively or destructively at the receiver, i.e. determine whether the scattering object counts as EEPS or not. Thus, only the dominant scatterers contribute to the richness.

The dependency on position can be observed even for distances that are fractions of the wavelength. One example is given in Fig. 4. There two arrays are compared that are shifted in position by half a wavelength. Obviously, the richness spectra are significantly influenced by the shift in position. However, it can still be observed that both spectra are strongly correlated, i.e. the maxima and minima occur at similar frequencies.

IV. CONCLUSIONS

The theoretical predictions derived from random matrix theory in [1] have been shown to accurately match measurement data. Even the assumption of identical path delays leads to only minor deviations between theoretical predictions and indoor propagation conditions in terms of eigenvalue distributions of the channel's covariance matrix. In addition the number of equivalent equal power scatterers was found to strongly

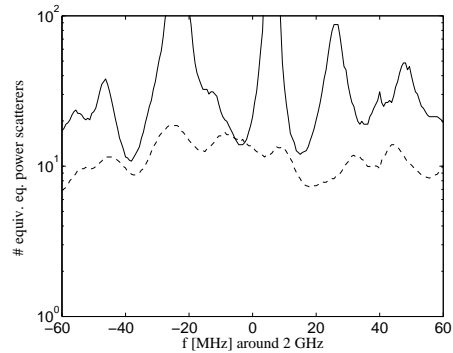


Fig. 4: The solid line shows the richness spectrum measured with tin foil and a 7-element uniform linear transmit array spaced a hole wavelength. The dashed line shows the richness spectrum measured after the position of the array has been shifted by half a wavelength.

vary with frequency. Therefore, a frequency hopping strategy can be helpful to achieve rich scattering, in practice.

ACKNOWLEDGMENT

The authors would like to thank C. Mecklenbräuker, K. Kopsa, H. Kunczler, M. Lončar, Siemens AG, Austria, and T-Nova GmbH.

REFERENCES

- [1] R.R. Müller. A random matrix model of communication through antenna arrays. In *Proc. of 38th Ann. Allerton Conf. Commun., Control & Comp.*, Monticello, IL, Oct. 2000.
- [2] G. J. Foschini. Layered space-time architecture for wireless communication in a fading environment when using multi-element antennas. *Bell Labs Techn. J.*, 1(2):41-59, 1996.
- [3] G. G. Raleigh and J. M. Cioffi. Spatio-temporal coding for wireless communication. *IEEE Trans. Commun.*, 46(3):357-366, Mar. 1998.
- [4] H. Bölcskei, D. Gesbert, and A. J. Paulraj. On the capacity of wireless systems employing OFDM-based spatial multiplexing. *Submitted to IEEE Trans. Commun.*, Oct. 1999.
- [5] D. V. Voiculescu, K. J. Dykema, and A. Nica. *Free Random Variables*. American Mathematical Society, Providence, RI, 1992.
- [6] I. E. Telatar. Capacity of multi-antenna Gaussian channels. *European Trans. Telecommun.*, 10(6), Nov/Dec. 1999.
- [7] J. B. Andersen. Antenna arrays in mobile communications: Gain, diversity, and channel capacity. *IEEE AP-Mag.*, 42(2):12-16, Apr. 2000.
- [8] M. Steinbauer, D. Hampicke, G. Sommerkorn, A. Schneider, A. F. Molisch, R. Thomä, and E. Bonek. Array measurement of the double-directional mobile radio channel. In *Proc. of IEEE VTC*, Tokyo, Japan, May 2000.
- [9] M. Steinbauer et al. COST 259 SWG 2.1 Mission Report: Modelling Unification Workshop. COST259 TD(99) 061.